COMMUNICATION

The Effective Conjugation Length is Responsible for the Red/Green Spectral Tuning in the Cyanobacteriochrome Slr1393g3

Christian Wiebeler, Aditya G. Rao, Wolfgang Gärtner and Igor Schapiro*

Abstract: The origin of the spectral shift from a red- to a green-absorbing form in a cyanobacteriochrome, Slr1393g3, is identified by application of combined quantum mechanics/molecular mechanics simulations. This protein, related to classical phytochromes, carries the open-chain tetrapyrrole chromophore phycocyanobilin. Our calculations reveal that the effective conjugation length in the chromophore becomes shorter upon conversion from the red to the green form. This is related to the planarity of the entire chromophore. A large distortion is found for the terminal pyrrole rings A and D, however, the D ring contributes stronger to the photoproduct tuning, despite a larger change in the twist of the A ring. Our findings implicate that the D ring twist can be exploited to regulate absorption of the photoproduct. Hence, mutations that affect the D ring twist can lead to rational tuning of the photoproduct absorption that allows tailoring of cyanobacteriochromes for biotechnological applications such as optogenetics and bioimaging.

Phytochromes are a widespread family of responsive photoreceptors initially discovered in plants.[1] Canonical phytochromes utilize covalently attached bilin chromophores that enable a reversible photoconversion between red (P_r) and far-red absorbing (P_{fr}) forms. Recently, a new subgroup of the phytochrome superfamily called cyanobacteriochromes (CBCRs) was found in cyanobacteria.[2–4] Despite the phylogenetic relation to canonical phytochromes, the CBCR family stands out by the compact protein size, as they maintain the salient features of phytochromes (autocatalytic chromophore binding, photochromicity) in a single GAF domain contrasting the PAS-GAF-PHY architecture of canonical phytochromes. More importantly, CBCRs exhibit an unprecedented diversity in the spectral tuning spanning the entire visible spectrum and its extension from near-IR to the near-ultraviolet region.[2,5–7] One frequently present subfamily of CBCRs exhibits a red-absorbing dark state (P_r) and a green-absorbing photoproduct state (P_g) showing a shift in absorption of more than 100 nm (Fig. 1B).[8] Thus, the photoproduct absorption undergoes a hypsochromic shift instead of the bathochromic one in canonical phytochromes. This leads to the question about the factors that trigger such a reverse shift. An understanding of the spectral tuning mechanism will pave the way for biotechnological applications like optogenetics and super-resolution microscopy, where CBCRs are promising candidates due to their compact size and spectral diversity.[9,10] In the present work we explain this spectral tuning mechanism for a representative CBCR protein by employing the hybrid quantum mechanics/molecular mechanics (QM/MM) method.

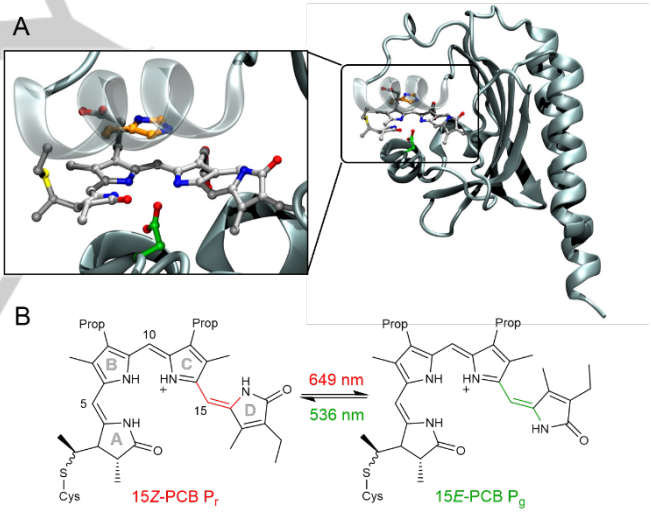

Figure 1. (A) Slr1393g3 protein structure in the P_r form. Zoom: The chromophore binding pocket. The PCB chromophore and the bound CYS-528 are shown with gray-colored carbon atoms, HIS-529 in orange and ASP-498 in green. The molecular structure was visualized using VMD.[11] (B) Schematic presentation of the PCB structures in both red- and green-absorbing forms. The differences between both forms are highlighted in red and green for P_r and P_g, respectively. The wavelengths refer to the lowest energy absorption maxima of the measured spectra.

Historically, four models were proposed to explain the blue shift from the P_r to the P_g form of CBCRs as reviewed by Lagarias and coworkers.[12] The "PCB/PVB-isomerization" model suggesting the isomerization of phycocyanobilin (PCB) to phycoviolobilin was only formally considered and ruled out on the experimental basis.[12] Also the "protochromic model"[8,13,14] which implies a change of PCB's protonation state either at the B- or the C-ring

Dr. C. Wiebeler, A. G. Rao, Dr. I. Schapiro
Fritz Haber Center for Molecular Dynamics Research
Institute of Chemistry
The Hebrew University of Jerusalem
Jerusalem 91904 (Israel)
E-mail: igor.schapiro@mail.huji.ac.il

Prof. Dr. W. Gärtner
Institut für Analytische Chemie
Fakultät für Chemie und Mineralogie
Universität Leipzig
D-04103 Leipzig (Germany)

Supporting information for this article is given via a link at the end of the document.

was recently discarded on the basis of resonance Raman and NMR studies.[15–17] These spectroscopic results provided evidence for a fully protonated chromophore in both forms. The two remaining tuning mechanisms are the "solvatochromic model" and the "trapped-twist model". The former is a collective term for various possible changes in the PCB environment. Hildebrandt and coworkers have attributed it to a change in the hydration of the PCB binding pocket,[15] while Matysik and coworkers have proposed protein interactions, in particular of charged amino acids, to cause the photoproduct tuning.[17,18] Charged amino acids are known to play a major role in the spectral tuning of the visual pigment rhodopsin, where the negatively charged glutamate counterion blue shifts the absorption of retinal by 120 nm (0.5 eV).[19] The "trapped-twist model" has been put forward based on experimental results by Lagarias and coworkers.[12,20–22] They postulate that PCB is significantly more twisted in P_g than in P_r form resulting in smaller effective conjugation lengths and therefore a blue shift in the absorption. Possible structural changes might involve either the twisting of the outer rings (A and/or D) or the entire chromophore.[12,14,17,20–23] Hence, our study focuses on a discrimination of these two models.

In the red/green CBCR subfamily, PCB is covalently bound to a cysteine residue as a chromophore. Upon light-absorption PCB isomerizes from 15-*Z* to 15-*E*. The photoisomerization shifts the absorption from red to green (Fig. 1B). Spectroscopic studies have been reported for several members of the red/green subfamily, i.e.: AnPixJg2,[9,13–15,17,18,23,24] NpR6012g4,[12,16,30,20–22,25–29] and Slr1393g3.[31–34] However, computational studies of the spectral tuning in this CBCR family and other related bilin-binding photoreceptors are rare[35–38] although the hybrid quantum mechanics/molecular mechanics (QM/MM) methodology has provided valuable insight into the spectral tuning of other photoreceptor protein families with isomerizable double bonds.[19,39–41] The simulations performed so far for CBCRs are either classical molecular dynamics of the protein[15,24] or excited state quantum chemical calculations on isolated chromophores.[21,36,42–46] A computational approach to describe the spectral properties of phytochromes and CBCRs was impaired not only by the size and flexibility of the chromophore but also by a lack of sufficiently resolved crystal structures. Only the crystal structure of the P_r form of AnPixJg2 was solved by Narikawa et al.[14] Recently, the crystal structures of both forms (P_r and P_g) of Slr1393g3 were deposited in the protein database.[47] These structures exhibit a PCB chromophore that is located in a protein cleft, covalently bound to CYS-528 and sandwiched between HIS-529 and ASP-498. The three aforementioned residues (Fig. 1A) form a central motif widely conserved among CBCRs and phytochromes. These key residues are instrumental for chromophore binding and maintenance of the spectral and photochemical properties.[14] Here we present accurate QM/MM simulations on the spectral tuning in the red/green CBCR representative Slr1393g3.

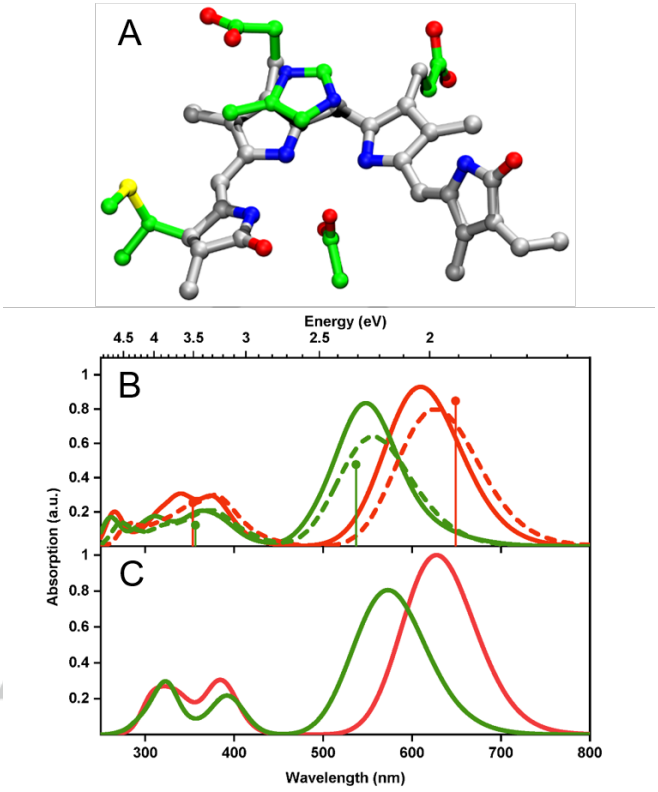

Figure 2. A) Composition of the QM regions. The smaller QM region (QM66) contains a truncated PCB chromophore. The extension to the larger region (QM106) is emphasized in green. B) Calculated absorption spectra of the P_g (green) and P_r (red) states: QM66 at the RI-ADC(2)/cc-pVDZ level of theory (solid) and QM106 at the RVS(50 eV)-RI-ADC(2)/cc-pVDZ level (dashed). The positions and the relative heights of the experimental absorption maxima[34] are indicated as sticks. C) Calculated absorption spectra of the QM66 model at the RI-ADC(2)/cc-pVDZ level of theory in absence of the protein environment for both forms.

The computations were based on the recently solved crystal structures of the P_r and P_g forms of Slr1393g3. The protein structures were solvated in a box with water, equilibrated and then subject to hybrid QM/MM calculations. Two different sizes of the QM region were tested: 66 and 106 atoms. The calculated absorption spectra in Fig. 2 are based on the *ab initio* method RI-ADC(2) applied to 100 snapshots from QM/MM molecular dynamics simulations (see Computational Details, Supporting Information). For the QM66 model we find a spectral shift of 0.23 eV, in qualitative agreement with the experimentally determined value of 0.40 eV. In the calculated spectrum the lowest energy absorption maximum of the P_r form is found at 610 nm (2.03 eV), blue shifted by 0.12 eV relative to the experimental absorption maximum at 649 nm (1.91 eV), (Fig. 2 B). The corresponding maximum of P_g is located at 548 nm (2.26 eV), red shifted by 0.05 eV compared to the experimental value of 537 nm (2.31 eV). Furthermore, the relative intensities of the first band follow the same trend as the measured ones. In addition to the lowest energy absorption band, our simulations also provide

absorption bands at higher energies. Their positions and relative intensities are in qualitative agreement with the experiment.

First, we address the "solvatochromic model" where the protein or a change in the solvation is proposed to tune the excitation energies. This model can be probed by varying the size of the QM region. A minimal QM region of the truncated PCB (QM66) was compared to the full chromophore including the three conserved residues (QM106, Fig. 2A). The spectra in Fig. 2B indicate that the size of the QM region does not affect the extent of the spectral shift, as it is 0.25 eV for the larger model compared to 0.23 eV for the smaller one. Subsequently we computed the spectra for the isolated chromophore in the strained geometry induced by the protein. This was performed by neglecting the environment in the excitation energy calculations and comparing the results to the protein-embedded calculations. For this comparison, the smaller QM66 model was applied because it allows to clearly separate between the protein and the chromophore. As shown in Fig. 2C, this leads to a small red shift in the averaged absorption spectra. However, this P_g-P_r shift is consistent because the difference is 0.19 eV, compared to the 0.23 eV obtained for the protein embedding. Therefore, we conclude that the main contribution to the photoproduct tuning does not originate from a direct electrostatic effect. Instead, the protein is imposing a steric constraint resulting in a distorted PCB chromophore geometry. This is in line with results by González and coworkers for the chromophore of phytochromes.[36,37] These authors report that excitation energy calculations based on X-ray geometries yield better agreement with experimental absorption spectra than freely optimized PCB structures *in vacuo*. Such chromophore distortions are the basis of the "trapped-twist model" by Lagarias and coworkers.[12,20–22]

To pinpoint the origin of the tuning mechanism, the twisting of the outer rings (A and D) relative to the central rings B and C, quantified by the angles Φ_{AB} and Φ_{CD} was evaluated (see Supporting Information). This analysis performed for each of the 100 snapshots is plotted for the S_1 excitation energies as a function of these two angles (Fig. 3). This plot indicates that the structures of P_g tend to exhibit a greater twisting of the outer rings, in particular for Φ_{AB} (Fig. S9), relative to P_r. It can be seen qualitatively that greater twist angles found in the P_g form result in higher excitation energies confirming its influence on the absorption energy. Indeed, Resonance Raman and NMR experiments on related red/green CBCRs confirm an increase of the twist along all three methine bridges in the P_g form with the largest increase between the A and B rings.[15,17,22] Interestingly, the Pearson correlation coefficient (0 = no correlation, 1 = ideal correlation) between the excitation energies and the tilting angle is higher for Φ_{CD} than Φ_{AB}. However, the former value is only 0.40 for P_g and even lower, 0.18, for P_r. This low correlation can be rationalized by the fact that, among other factors, ring puckering is not accounted for in our analysis.

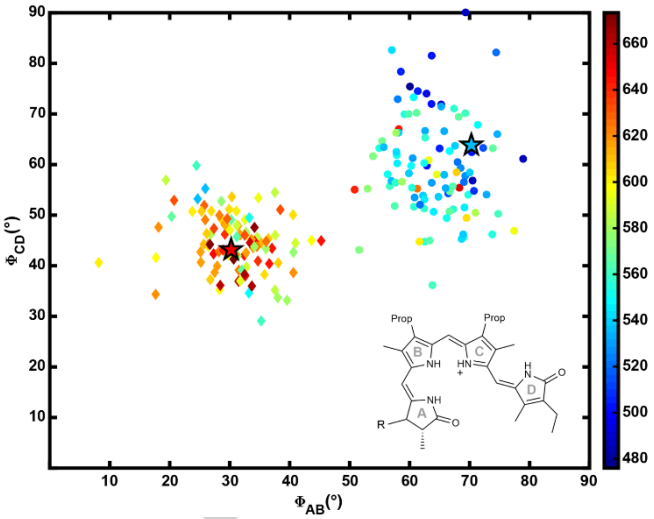

Figure 3. Scatter plot based on the tilting angles between rings A and B (Φ_{AB}) and between rings C and D (Φ_{CD}) in Slr1393. The absorption wavelength of the S_1 state is used for color coding. The P_r excitation energies are marked as diamonds, whereas P_g excitation energies are marked with circles. The experimental absorption maxima of both forms are shown as stars and the tilting angles are taken from the crystal structures.

However, instead of correlating further geometrical parameters with the excitation energy of the S_1 state we performed a detailed analysis of the electronic structure. To this end, the wave function analysis developed by Plasser et al. was employed.[48–50] This approach is based on partitioning the molecule into fragments and developing descriptors based on the decomposition of the one-particle transition density among these fragments (see the Supporting Information for further details). In our case, one descriptor is of particular interest: the delocalization length (DL), originally introduced in a study of polyadenine.[51] This parameter describes how many fragments are involved in the excitation, e.g. a DL value of 1 corresponds to an excitation localized on one single fragment while the maximum DL value is the total number of fragments. For this analysis, the atoms of QM66 were divided into three fragments: (1) the A ring, (2) the B and C rings including all methine bridges, and (3) the D ring (see also Scheme S1). The choice of treating rings B and C as one fragment is motivated by their co-planarity, in contrast to the A and D rings.

Table 1. Statistics of the wave function analysis of the S_1 state for 100 snapshots of P_r (left) and P_g (right) forms. The excitation energies (ΔE in eV), oscillator strengths (f), and delocalization lengths (DL) are listed. The table presents mean values (Mean), standard deviations (Std) as well as maximum (Max.) and minimum (Min.) values.

	P_r				P_g			
	Mean	**Std**	**Max.**	**Min.**	**Mean**	**Std**	**Max.**	**Min.**
ΔE	2.04	0.10	2.32	1.84	2.27	0.14	2.61	1.90
f	1.05	0.08	1.24	0.88	1.04	0.11	1.35	0.75
DL	1.60	0.08	1.79	1.44	1.41	0.12	1.74	1.11

A statistical overview of the wave function analysis for 100 snapshots of each form in the S_1 state is given in Table 1. We note that the average values for the excitation energies closely match the positions of the simulated absorption maxima. It is apparent that the excitation is more delocalized for P_r than for P_g form with values of 1.60 and 1.41, respectively. Correlating DL with excitation energies results in correlation coefficients of around 0.78 for P_g and of 0.49 for P_r, which is significantly higher than the correlation of specific outer ring twisting angles with excitation energies. This is due to the fact that DL describes a collective structural deformation of the PCB

chromophore instead of selectively referring to one single structural parameter.

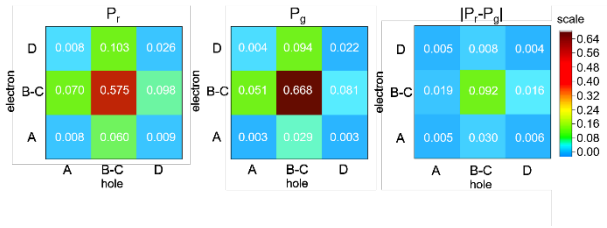

Figure 4. Electron-hole correlation plots of the average values of P_r (left), P_g (middle) and of the absolute value of the difference of these values (right) based on the S_1 states of 100 snapshots for each form. The scale for all plots is shown on the right.

Essential support for our calculations arrives from the plots of the averaged matrix of charge transfer numbers, called electron-hole correlation plots[49] (Fig. 4). Here, the excitation is first reduced to a two-particle picture: excited electron and hole. Then the probability of finding the excited electron (y-axis) and the hole in any of the three fragments (x-axis) is quantified. The plot demonstrates that the excitation is mainly localized on fragment 2 for both forms. However, the value is smaller for P_r (0.575) than for P_g (0.668). The next highest contributions in the electron-hole correlation plots originate from excitations between fragments 1 or 3 on the one hand and fragment 2 on the other. Here the relation is the other way around: the inter-fragment contributions are larger for P_r than for P_g. Both findings are consistent with the DL analysis. The lowest contributions are coming from local excitations on fragment 1 or 3 and from inter-fragment excitations among them, which are found to be negligible.

To conclude, based on the recently determined crystal structures of the red-/green-absorbing CBCR Slr1393g3 we have simulated spectra and could reproduce the absorption bands of both forms over the entire wavelength range down to 300 nm. The analysis yields an understanding of the spectral tuning of the first absorption band on a molecular level. Turning off the electrostatic effect of the environment, represented by point charges, does not significantly alter the difference in absorption between the two forms. Hence, this finding rules out the “solvatochromic model” for spectral tuning. Further, our analysis of the chromophore geometry and of the wave functions identifies the twist of the A and D rings relative to the B and C rings as the origin of the tuning. These findings are in line with the empirically proposed “trapped twist” mechanism and spectroscopic studies. The wave function analysis clearly demonstrates that the effective length of the conjugated system is the dominating factor for the photoproduct tuning. The extent of the contribution depends on the planarity of the entire PCB chromophore. To describe this appropriately, descriptors like the DL value have proven useful tools, as confirmed by its relatively high correlation. Although the change of the twist of the A ring is higher than of the D ring, it is this latter one that determines the photoproduct tuning. In contrast, the absorption in the dark state is less correlated with the out of plane movement of the D ring. The implication of our finding is that further D ring twist would blue shift the photoproduct absorption while reducing it would result in a red shift. Hence, mutations that affect the D ring twist can lead to rational tuning of the photoproduct absorption.

Acknowledgements

This project has received funding from the European Research Council (ERC) under the European Union’s Horizon 2020 research and innovation programme (grant agreement No 678169, ERC Starting Grant "PhotoMutant”). I.S. is grateful for the Mercator Fellowship and the support from the DFG (Grant No. SFB 1078). C.W. acknowledges support by the German Research Foundation (DFG) via a research scholarship (reference number: WI 4853/1-1). The Turbomole calculations leading to the results presented here were performed on resources provided by the Paderborn Center for Parallel Computing.

Keywords: Spectral Tuning • Hybrid QM/MM • Cyanobacteriochrome • Tetrapyrrole • Chromophore

[1] N. C. Rockwell, Y.-S. Su, J. C. Lagarias, *Annu. Rev. Plant Biol.* **2006**, *57*, 837–858.

[2] M. Ikeuchi, T. Ishizuka, *Photochem. Photobiol. Sci.* **2008**, *7*, 1159–1167.

[3] C. Heintzen, *WIREs Membr. Trans. Signal.* **2012**, *1*, 411–432.

[4] N. C. Rockwell, R. Ohlendorf, A. Möglich, *Proc. Natl. Acad. Sci. USA* **2013**, *110*, 806–807.

[5] N. C. Rockwell, S. S. Martin, K. Feoktistova, J. C. Lagarias, *Proc. Natl. Acad. Sci.* **2011**, *108*, 11854–11859.

[6] G. Enomoto, Y. Hirose, R. Narikawa, M. Ikeuchi, *Biochemistry* **2012**, *51*, 3050–3058.

[7] N. C. Rockwell, S. S. Martin, A. G. Gulevich, J. C. Lagarias, *Biochemistry* **2012**, *51*, 1449–1463.

[8] N. C. Rockwell, S. S. Martin, J. C. Lagarias, *Biochemistry* **2012**, *51*, 9667–9677.

[9] K. Fushimi, G. Enomoto, M. Ikeuchi, R. Narikawa, *Photochem. Photobiol.* **2017**, *93*, 681–691.

[10] O. S. Oliinyk, K. G. Chernov, V. V. Verkhusha, *Int. J. Mol. Sci.* **2017**, *18*, 1691.

[11] W. Humphrey, A. Dalke, K. Schulten, *J. Mol. Graph.* **1996**, *14*, 33–38.

[12] N. C. Rockwell, S. S. Martin, A. G. Gulevich, J. C. Lagarias, *Biochemistry* **2014**, *53*, 3118–3130.

[13] Y. Fukushima, M. Iwaki, R. Narikawa, M. Ikeuchi, Y. Tomita, S. Itoh, *Biochemistry* **2011**, *50*, 6328–6339.

[14] R. Narikawa, T. Ishizuka, N. Muraki, T. Shiba, G. Kurisu, M. Ikeuchi, *Proc. Natl. Acad. Sci.* **2013**, *110*, 918–923.

[15] F. Velazquez Escobar, T. Utesch, R. Narikawa, M. Ikeuchi, M. A. Mroginski, W. Gärtner, P. Hildebrandt, *Biochemistry* **2013**, *52*, 4871–4880.

[16] N. C. Rockwell, S. S. Martin, S. Lim, J. C. Lagarias, J. B. Ames, *Biochemistry* **2015**, *54*, 2581–2600.

[17] C. Song, F. Velazquez Escobar, X. L. Xu, R. Narikawa, M. Ikeuchi, F. Siebert, W. Gärtner, J. Matysik, P. Hildebrandt, *Biochemistry* **2015**, *54*, 5839–5848.

[18] C. Song, R. Narikawa, M. Ikeuchi, W. Gärtner, J. Matysik, *J. Phys. Chem. B* **2015**, *119*, 9688–9695.

[19] S. Sekharan, M. Sugihara, V. Buss, *Angew. Chemie - Int. Ed.* **2007**, *46*, 269–271.

[20] N. C. Rockwell, S. S. Martin, F. Gan, D. A. Bryant, J. C. Lagarias, *Photochem. Photobiol. Sci.* **2015**, *14*, 258–269.

[21] N. C. Rockwell, S. S. Martin, S. Lim, J. C. Lagarias, J. B. Ames, *Biochemistry* **2015**, *54*, 3772–3783.

[22] S. Lim, Q. Yu, S. M. Gottlieb, C.-W. Chang, N. C. Rockwell, S. S. Martin, D. Madsen, J. C. Lagarias, D. S. Larsen, J. B. Ames, *Proc. Natl. Acad. Sci.* **2018**, 201720682.

[23] R. Narikawa, Y. Fukushima, T. Ishizuka, S. Itoh, M. Ikeuchi, *J. Mol. Biol.* **2008**, *380*, 844–855.

[24] L. K. Scarbath-Evers, S. Jähnigen, H. Elgabarty, C. Song, R. Narikawa, J. Matysik, D. Sebastiani, *Phys. Chem. Chem. Phys.* **2017**, *19*, 13882–13894.

[25] P. W. Kim, L. H. Freer, N. C. Rockwell, S. S. Martin, J. C. Lagarias, D. S. Larsen, *Biochemistry* **2012**, *51*, 608–618.

[26] P. W. Kim, L. H. Freer, N. C. Rockwell, S. S. Martin, J. C. Lagarias, D. S. Larsen, *Biochemistry* **2012**, *51*, 619–630.

[27] P. W. Kim, L. H. Freer, N. C. Rockwell, S. S. Martin, J. C. Lagarias, D. S. Larsen, *J. Am. Chem. Soc.* **2012**, *134*, 130–133.

[28] C.-W. Chang, S. M. Gottlieb, P. W. Kim, N. C. Rockwell, J. C. Lagarias, D. S. Larsen, *J. Phys. Chem. B* **2013**, *117*, 11229–11238.

[29] S. Lim, Q. Yu, N. C. Rockwell, S. S. Martin, J. Clark Lagarias, J. B. Ames, *Biomol. NMR Assign.* **2016**, *10*, 157–161.

[30] Q. Yu, S. Lim, N. C. Rockwell, S. S. Martin, J. Clark Lagarias, J. B. Ames, *Biomol. NMR Assign.* **2016**, *10*, 139–142.

[31] Y. Chen, J. Zhang, J. Luo, J. M. Tu, X. L. Zeng, J. Xie, M. Zhou, J. Q. Zhao, H. Scheer, K. H. Zhao, *FEBS J.* **2012**, *279*, 40–54.

[32] X.-L. Xu, A. Gutt, J. Mechelke, S. Raffelberg, K. Tang, D. Miao, L. Valle, C. D. Borsarelli, K.-H. Zhao, W. Gärtner, *ChemBioChem* **2014**, *15*, 1190–1199.

[33] F. Pennacchietti, A. Losi, X. Xu, K. Zhao, W. Gärtner, C. Viappiani, F. Cella, A. Diaspro, S. Abbruzzetti, *Photochem. Photobiol. Sci.* **2015**, *14*, 229–237.

[34] C. Slavov, X. Xu, K. H. Zhao, W. Gärtner, J. Wachtveitl, *Biochim. Biophys. Acta - Bioenerg.* **2015**, *1847*, 1335–1344.

[35] S. Gozem, H. L. Luk, I. Schapiro, M. Olivucci, *Chem. Rev.* **2017**, *117*, 13502–13565.

[36] R. A. Matute, R. Contreras, G. Pérez-Hernández, L. González, *J. Phys. Chem. B* **2008**, *112*, 16253–16256.

[37] R. A. Matute, R. Contreras, L. González, *J. Phys. Chem. Lett.* **2010**, *1*, 796–801.

[38] O. Falklöf, B. Durbeej, *J. Comput. Chem.* **2013**, *34*, 1363–1374.

[39] L. V. Schäfer, G. Groenhof, A. R. Klingen, G. M. Ullmann, M. Boggio-Pasqua, M. A. Robb, H. Grubmüller, *Angew. Chemie - Int. Ed.* **2007**, *46*, 530–536.

[40] P. Campomanes, M. Neri, B. A. C. Horta, U. F. Röhrig, S. Vanni, I. Tavernelli, U. Rothlisberger, *J. Am. Chem. Soc.* **2014**, *136*, 3842–3851.

[41] C. Cheng, M. Kamiya, Y. Uchida, S. Hayashi, *J. Am. Chem. Soc.* **2015**, *137*, 13362–13370.

[42] C. Zazza, N. Sanna, M. Aschi, *J. Phys. Chem. B* **2007**, *111*, 5596–5601.

[43] N. C. Rockwell, S. L. Njuguna, L. Roberts, E. Castillo, V. L. Parson, S. Dwojak, J. C. Lagarias, S. C. Spiller, *Biochemistry* **2008**, *47*, 7304–7316.

[44] N. C. Rockwell, L. Shang, S. S. Martin, J. C. Lagarias, *Proc. Natl. Acad. Sci.* **2009**, *106*, 6123–6127.

[45] A. Strambi, B. Durbeej, *Photochem. Photobiol. Sci.* **2011**, *10*, 569–579.

[46] Y. Yang, M. Linke, T. von Haimberger, R. Matute, L. González, P. Schmieder, K. Heyne, *Struct. Dyn.* **2014**, *1*, 014701.

[47] X. Xu, A. Port, C. Wiebeler, K.-H. Zhao, I. Schapiro, W. Gärtner, under review.

[48] F. Plasser, H. Lischka, *J. Chem. Theory Comput.* **2012**, *8*, 2777–2789.

[49] F. Plasser, M. Wormit, A. Dreuw, *J. Chem. Phys.* **2014**, *141*, 024106.

[50] F. Plasser, S. A. Bäppler, M. Wormit, A. Dreuw, *J. Chem. Phys.* **2014**, *141*, 024107.

[51] J. J. Nogueira, F. Plasser, L. González, *Chem. Sci.* **2017**, *8*, 5682–5691.

Entry for the Table of Contents (Please choose one layout)

COMMUNICATION

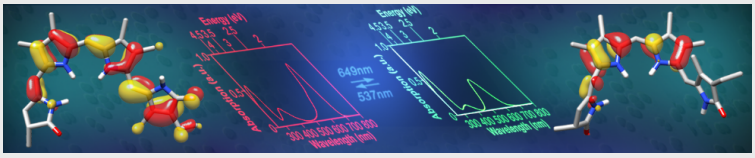

*Author(s), Corresponding Author(s)**

Page No. – Page No.

Title

The origin of the spectral shift from a red- to a green-absorbing form in a cyanobacteriochrome, Slr1393g3, is identified by application of combined quantum mechanics/molecular mechanics simulations and wave function analysis. Our calculations reveal that the effective conjugation length in the chromophore becomes shorter upon conversion from the red to the green form.